Organic Electronics 15 (2014) 3648–3653

Contents lists available at ScienceDirect

Organic Electronics

journal homepage: www.elsevier.com/locate/orgel

Tunable microcavities in organic light-emitting diodes by way of low-refractive-index polymer doping

An-Kai Ling [a,b], Chun-Hao Lin [a,c], Hsun Liang [a,c], Fang-Chung Chen [a,b,*]

[a] Department of Photonics, National Chiao Tung University, Hsinchu 30010, Taiwan
[b] Institute of Display, National Chiao Tung University, Hsinchu 30010, Taiwan
[c] Institute of Electro-optical Engineering, National Chiao Tung University, Hsinchu 30013, Taiwan

ARTICLE INFO

Article history:
Received 9 September 2014
Received in revised form 6 October 2014
Accepted 10 October 2014
Available online 28 October 2014

Keywords:
Organic
Light-emitting
Microcavity
Refractive index
Resonant

ABSTRACT

A method for enhancing the light out-coupling efficiency of organic light-emitting devices (OLEDs) has been demonstrated by blending a low-refractive-index polymer, poly(2,2,3,3,3-pentafluoropropyl methacrylate) (PPFPMA), into the emission layer. The resonant wavelength of the weak microcavity devices blueshifted accompanied with a decrease in refractive indices of the light-emitting layers after the addition of PPFPMA. Stronger directed emission toward the surface normal was obtained when the resonant wavelength became closer to the peak wavelength of intrinsic emission spectrum of the organic emitters. The luminous efficiency of the devices was enhanced by more than 20%. The results suggest that the microcavity properties of the OLEDs can be tunable through blending low-refractive-index materials.

1. Introduction

Organic light-emitting diodes (OLEDs) are playing an increasingly conspicuous role in the next generation display and solid-state lighting technologies because of their high efficiencies, low cost, and their potential to act as large-area and flexible devices [1–3]. Meanwhile, nearly 100% internal quantum efficiencies have been realized by doping phosphorescent molecules to harvest triplet excitons [4,5]. Nevertheless, because of the mismatch of the refractive indices, a large proportion of the generated photons is trapped in the devices and the light out-coupling efficiency (η_{out}) of conventional OLEDs is limited at *ca.* 20% [6]. Therefore, substantial enhancement in the light extraction efficiencies will be necessary if we are to further improve the device efficiencies.

Many approaches, including using high-refractive-index substrates [3,7], microlense arrays [8,9], photonic crystals [10], and plasmonic nanostructures [11], have been studied to enhance η_{out}. Meanwhile, the conventional structure of OLEDs naturally behaves as a weak microcavity because the dimension of their functional layers is similar to the wavelength of the emitting photons. While both electrodes exhibit high reflectivities, strong microcavity effects can be observed. Therefore, the microcavity effects redistribute the optical modes in the devices, and the η_{out} can be enhanced along the normal emission direction under certain conditions [12–18]. For instance, better light extraction can be achieved by setting the resonant wavelength of the cavity near the peak wavelength (λ_{em}) of the intrinsic emission spectrum [$S(\lambda)$] of the organic emitters [13,14]. To the best of our knowledge, however, most studies adjust the optical cavity length (L) of the microcavities through altering the thickness (d) of the organic layers [17,18]. No report tunes the values of L, which are equal to the products of the refractive indices [$n(\lambda)$] and d, by altering the refractive indices of the

* Corresponding author at: Department of Photonics, National Chiao Tung University, Hsinchu 30010, Taiwan. Tel.: +886 3 5131484; fax: +886 3 5735601.
E-mail address: fcchen@mail.nctu.edu.tw (F.-C. Chen).

http://dx.doi.org/10.1016/j.orgel.2014.10.013
1566-1199/

emission layers. Adjusting the values of L through varying the thicknesses of the active layers, however, inevitably affects other electrical properties, such as the internal electrical field strength and the width and location of the recombination zone, resulting in a rather complicated situation for structure designs [19]. An alternative way is to change the refractive indices of the emission layers. In this work, we demonstrated a simple, effective method for enhancing η_{out} of polymer light-emitting diodes (PLEDs) by blending a low-refractive-index polymer, poly(2,2,3,3,3-pentafluoropropyl methacrylate) (PPFPMA), into the emission layer. The microcavity effects of the devices can be optimizing by tuning the $n(\lambda)$ of the emission layer with the amount of PPFPMA. As a result, the luminous efficiency incorporating PPFPMA was enhanced by approximately 20%.

2. Experimental

Fig. 1 shows the device structure and the chemical structures of the materials used in this work. For device fabrication, indium tin oxide (ITO)-coated glass substrates were cleaned with detergent, followed by sequential sonication in deionized water, acetone, and isopropanol. They were then dried in an oven overnight. Prior to use, the substrates were further treated with UV-ozone. Poly(3,4-ethylenedioxythiophene)–poly(styrenesulfonate) (PEDOT:PSS) was spin coated onto the ITO substrates and then baked at 120 °C for 1 h. The emission layer comprised poly(vinylcarbazole) (PVK), 2-(4-biphenyl)-5-(4-tert-butyl-phenyl)-1,3,4-oxadiazole (PBD), and tris[2-(4-tolyl)phenylpyridine]iridium [Ir(mppy)$_3$] at a weight ratio of PVK:PBD:Ir(mppy)$_3$ = 70:29:1 [20–22]. The emission layer was deposited on top of the PEDOT:PSS layer from a solution of 1,2-dichlorobenzene inside a N_2-filled glovebox. The polymer film was then annealed at 80 °C for 30 min. To complete the devices, a cathode comprising 30 nm Ca and 100 nm Al was thermally deposited under a vacuum of *ca.* 5×10^{-6} Torr. The control devices were defined as those prepared without PPFPMA. For the devices containing PPFPMA, the low-refractive-index polymer was blended into the emission layer at various weight of 0.1–0.5% (w/w). For example, 0.1% PPFPMA indicated that the weight ratio of the components in the emissive layer was PVK:PBD:Ir(mppy)$_3$:PPFPMA = 70:29:1:0.1. The refractive index of PPFPMA was 1.140, which was measured by using an ellipsometer (Sopra GES-5). The thicknesses of the emission layer prepared with and without the addition of PPFPMA were precisely controlled and all of them were almost identical (*ca.* 70 nm); the thicknesses were obtained by using an atomic force microscope (AFM). The electrical characteristics of the PLEDs were recorded by a Keithley 2400 source measure unit. The brightness and the electroluminescent (EL) spectra were measured by using a PR650 SpectraScan colorimeter. The photoluminescent (PL) spectra were obtained using an Ocean Optics HR4000CG-UV-NIR spectrometer. A N_2-laser was used as the light source. The reflectivity spectra were obtained using a Perkin Elmer UV–Vis Lambda 650 spectrometer. The viewing angle dependence of luminance was determined using a ConoScope™ (Autronic-Melchers, GmbH), where a measuring cone of 80° over an azimuthal angle range of 360° could be obtained. The thin film morphology was analyzed using a DI 3100 series AFM.

3. Results and discussion

Fig. 2(a) shows the current density–brightness–voltage (J–B–V) curves of the PLEDs containing various amount of PPFPMA. The turn-on voltage (V_T), defined for a luminance of 0.1 cd/m^2, was 4.6 V for the control device. The devices prepared with 0.1% and 0.2% PPFPMA exhibited almost identical electrical characteristics, suggesting that the addition of PPFPMA did not affect the electrical properties of the devices significantly. However, as the concentration of PPFPMA was increased beyond 0.2%, we could see that the current density started to decrease obviously. The values of V_T became 4.8 V for the devices containing 0.3% PPFPMA, respectively. The increase in V_T could be attributed to the insulating nature of PPFPMA. The electrical properties of the devices fabricated under different conditions are summarized in Table 1. Fig. 2(b) and (c) display the luminance efficiency–current density (η–J) and power efficiency–current density (L_P–J) curves of the PLEDs prepared with and without PPFPMA. The maximum η and L_P of the control device were 20.5 cd/A and 9.3 lm/W, respectively. After adding PPFPMA into the emission layer, substantial enhancement in the luminance efficiency and power efficiency could be obtained. Compared with the control device, the peak η of the device containing 0.2% PPFPMA increased approximately by 22% to the 25.1 cd/A. Meanwhile, the L_P was also enhanced to 11.4 lm/W while the driving voltage was not significantly affected by adding

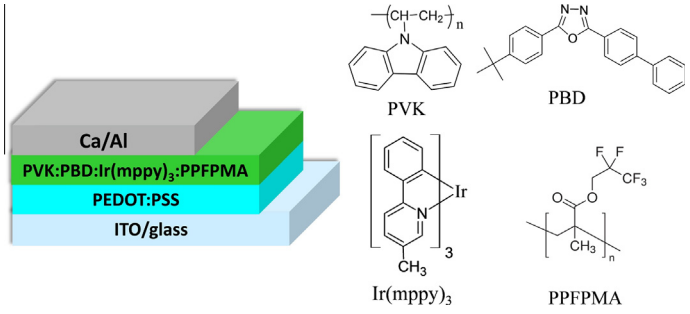

Fig. 1. Device structure and chemical structures of the organic materials used in this work.

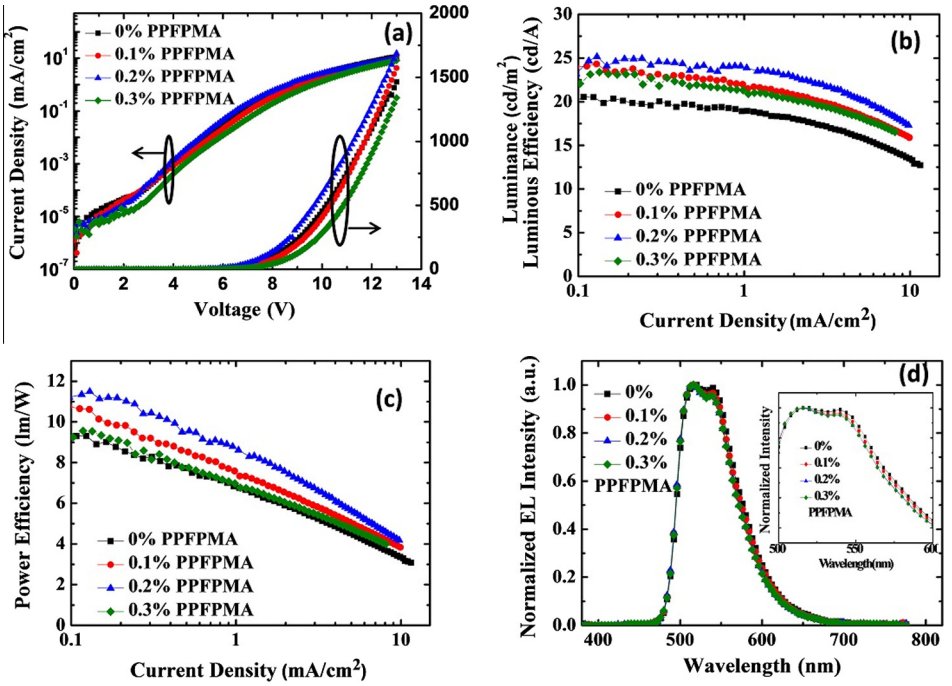

Fig. 2. (a) *J*–*L*–*V*; (b) L_E–*J*; (c) L_P–*J* characteristics of the devices fabricated with various amount of PPFPMA. (d) Normalized EL spectra of the devices prepared with and without the addition of PPFPMA; the inset shows the enlarged spectra in the wavelength range from 500 to 600 nm.

Table 1
Device characteristics of the PLEDs prepared with various PPFPMA concentrations.

Concentration (%) (w/w)[a]	Turn-on voltage (V)[b]	Max. luminance (cd/m^2)	Max. luminous efficiency (cd/A)	Max. power efficiency (lm/W)
0	4.5	1464	20.5	9.3
0.1	4.6	1573	24.0	10.8
0.2	4.6	1689	25.1	11.4
0.3	4.8	1339	23.4	9.6

[a] PVK:PBD:Ir(mppy)$_3$:PPFPMA = 70:29:1: weight ratio of PPFPMA.
[b] At 0.1 nits.

PPFPMA. Fig. 2(d) shows the EL spectra for the PLEDs fabricated with and without PPFPMA. The peak wavelength of the devices was 516 nm and stayed unchanged after the addition of PPFPMA, suggesting that the device enhancement was not due to the spectral change.

Because the optimal thickness of the photoactive films is in the order of a wavelength, a PLED can be considered as a one-dimensional microcavity. A cavity effect is governed mainly by wide-angle interference within the device; however, Fabry–Perot type multiple-beam resonance effect can also be present due to the low but finite reflection at glass/ITO interfaces [23]. In such structures, directly outgoing beams of the emission interfere with the beams reflected from the top metal cathode, thereby influencing the outcoupling intensity. From the optical point of view, a PLED can be treated as a planar Fabry–Perot microcavity. The resonant modes of a cavity should satisfy the condition that the phase change during one round trip is a multiple of 2π [24]. In other words, the following Eq. holds:

$$\sum_i \frac{4\pi \cos\beta}{\lambda} d_i n_i(\lambda) - \varphi_{top}(\beta,\lambda) - \varphi_{bot}(\beta,\lambda) = 2m\pi \qquad (1)$$

where λ is the resonance wavelength; m is an integer (0, 1, 2,...) that defines the mode number; $\varphi_{top}(\lambda)$, $\varphi_{bot}(\lambda)$ are the wavelength-dependent phase changes upon reflection from the top and bottom mirrors, respectively. The summation is performed over constituent organic layers inside the microcavity with thicknesses d_i and refractive indices $n_i(\lambda)$. The viewing angle is also incorporated, where β is the internal angle inside the cavity and is related to the external viewing angle α through the Snell's law: $n_{air}\sin(\alpha) = n_{cav}\sin(\beta)$. From Eq. (1), it is obvious that the resonance wavelengths of a microcavity can be tuned by altering the optical path length, i.e., the refractive indices and thicknesses of the organic layers, including those of the PEDOT:PSS buffer and the emission layers. In this work, the thicknesses of PEDOT:PSS and active polymer layers were kept constant during our investigation. Therefore, we inferred that the resonance wavelengths of the cavity were changed after blending the low-refractive-index polymers into the emissive layer. As a result, the η_{out} was enhanced along the normal emission direction after the nature of the weak microcavity was modified.

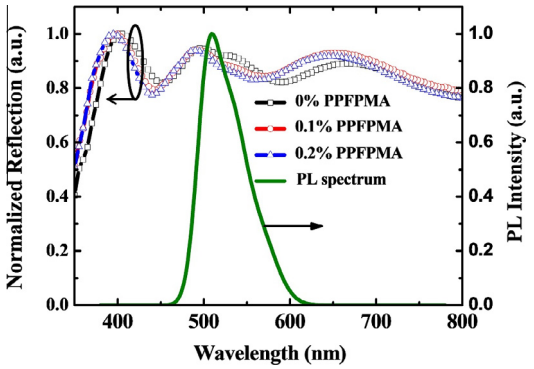

Fig. 3. Reflectivity spectra for the devices prepared with various amount of PPFPMA. The PL spectrum of the light-emitting polymer is also displayed.

In order to characterize the properties of the microcavity, the reflectivity spectroscopy was used [19,24]. Fig. 3 shows the reflectivity spectra in normal direction for the PLED devices prepared with different amount of PPFPMA. We observed two dips around 450 and 560 nm for the control device. Note that the absorption of ITO resulted in a dramatic decrease of the reflectivity at 350 nm. In principle, the presence of a dip in the reflectivity spectrum can be contributed to the interference effect and its location indicates the resonance wavelength. Further, because the weak microcavity of the PLEDs acts as a filter, the photons whose wavelength range falls outside of the dips are trapped in the cavity [19]. In our cases, the normal direction resonance wavelength λ_R (0°) was 590 nm for the control device and shifted to 570 and 560 nm for the device containing 0.1% and 0.2% PPFPMA, respectively (Fig. 3). Moreover, the PL spectrum of the light-emitting layer investigated in this work, which is the intrinsic spectral distribution of the organic emitters, is also shown in Fig. 3. The λ_R (0°) of the 0.2% PPFPMA device shifted by 30 nm relative to that of the control device and became more closed to the intrinsic emitting wavelength of the organic emitters. Because of the interference effect, substantial enhancement in forward luminance was achieved, resulting in a higher light out-coupling efficiency. Further, the EL spectra as displayed in Fig. 2(d) suggested that the portion of photons at 516 nm relatively increased after the use of PPFPMA. The intensity of the PL shoulder, which is centered at *ca.* 540 nm, relatively decreased because of the change of resonance conditions in the weak microcavities. These spectral results also support that the addition of the PPFPMA modified the microcavity properties of the devices.

The luminance of the PLEDs measured on Conoscope™ as a function of various viewing angles was shown in Fig. 4. Fig. 4(a)–(c) reveal the luminance contour plots of the devices prepared with various amount of PPFPMA.

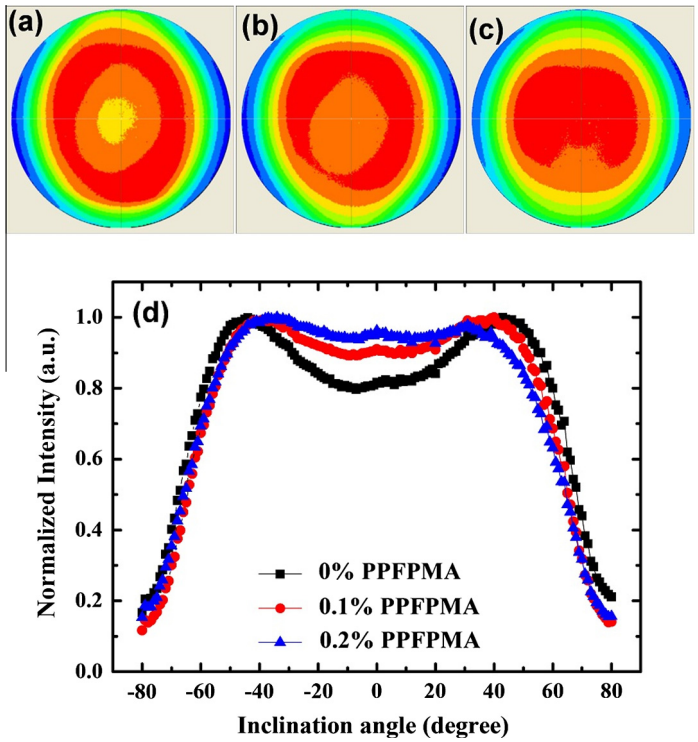

Fig. 4. Viewing angle dependences of the luminance of the PLEDs prepared (a) without PPFPMA, (b) with 0.1% PPFPMA, and (c) with 0.2% PPFPMA at constant current density of 0.2 mA/cm^2. The inclination and azimuthal angles were measured from 0° to 80° and 0° to 360°, respectively. The corresponding luminance (normalized to the maximum intensity) at 0° and 180° azimuthal angle and at different inclination angles was also shown in (d). Note that the luminance distribution was noncircular in symmetry due to the rectangular shape of the PLEDs. In other words, a *Lambertian* profile is corresponding to a flat line for all angles.

Inclination and azimuthal angles were measured from 0° to 80°and 0° to 360°, respectively. The luminance distribution was noncircular in symmetry because of the rectangular shape of the PLEDs; the active area was 0.1 cm^2 (0.2 cm × 0.5 cm) [9]. The corresponding luminance at 0° to 180° azimuthal angle and at different inclination angles was also revealed in Fig. 4(d); each curve was normalized to the maximum intensity of itself. Interestingly, the emission pattern exhibited the highest intensity at an off-axis angle of 40–50° and a relatively weak intensity in the forward direction. Similar patterns have been reported previously and attributed to the microcavity effect [19]. The changes of the angle profiles were due to the shift of the reflectivity dip with the viewing angle both in wavelength and in magnitude corresponding to their overlaps with the emission spectrum of the organic emitters [19]. In addition, from the reflectivity spectra, we could also realized that the unusual pattern was due to the large mismatch between the resonance conditions and the intrinsic light-emitting wavelength of the polymers. According to Eq. (1), we could also see that the location of the dip in reflectivity varies with the internal angle inside the cavity, which is closely related to the viewing angle. For the control device, the wavelength minimum at 590 nm blue-shifted to 545 nm while the viewing angle changed from 0° to 40°. Therefore, the overlap of the dip in reflectivity with the emission spectrum, in which the peak wavelength was 510 nm, became less at 0° viewing angle (Fig. 3), resulting in a lower luminance. On the other hand, the dip shifted closer to the intrinsic emission wavelength at higher angles, resulting in a peak luminance at viewing angles of 40–50°. As displayed in Fig. 4(d), the device prepared with 0.2% PPFPMA displayed stronger directed emission toward the surface normal and showed emission patterns more close to the *Lambertian* distribution. In short, the angle dependence of the device emission further confirmed the importance of the microcavity effects.

The interface between the polymer and the cathode plays an important role in determining the electrical characteristics of devices [2]. In order to investigate the influence of PPFPMA on the polymer film, the surface morphology of the composite films was analyzed by AFM. The height images of the active films before and after the addition of PPFPMA are displayed in Fig. 5. We observed that the surfaces of these films were very smooth. The surface roughness of the polymer film containing 0.1% PPFPMA was even decreased slightly. The almost identical morphology suggested no serious phase separation. Therefore, the addition of PPFPMA had little influence on the morphology of thee the films, revealing that the device improvements should be largely due to the optical effects.

Recently, phosphorescent dyes have been reported to have preferred horizontal dipoles, which could result in higher coupling efficiencies [25,26]. In our present work, we cannot completely rule out the possibility that the addition of PPFPMA might change the orientation of the dipoles. However, we consider the chance should be very limited because the amount of PPFPMA in the active films was low (0.1–0.3% in weight). We could not find any signature of dipole changes from our preliminary results, such as the absorption spectra. Further studies, such as angle-dependent PL measurements, are ongoing.

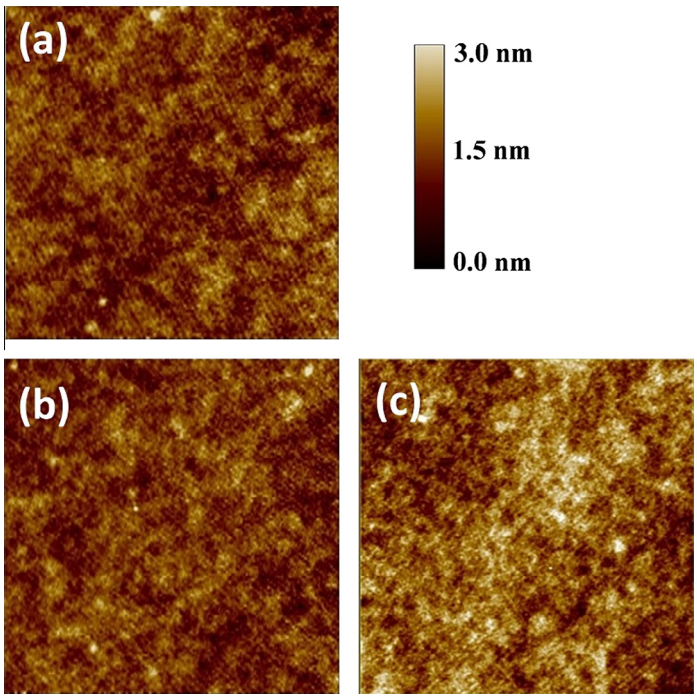

Fig. 5. AFM images of light-emitting polymer films prepared (a) without PPFPMA, (b) with 0.1% PPFPMA, and (c) with 0.2% PPFPMA. The image dimension is 5 × 5 μm.

4. Conclusions

We have demonstrated that the out-coupling efficiency of PLEDs can be enhanced by blending low-refractive-index polymers into the emission layer. Stronger directed emission toward the surface normal was obtained, leading to an efficiency enhancement of about 22%. The device improvement originated from the optimization of optical microcavity effects by adjusting the refractive indices of the emission layers after the addition of PPFPMA. The device prepared with 0.2% PPFPMA exhibited almost identical electrical characteristics and showed emission patterns more close to the *Lambertian* distribution. While the tuning of resonance conditions in OLEDs was achieved largely through changing the thickness of the functional layers, this work suggests that it can be also accomplished by altering the refractive indices of the emission layers. This work provides a very convenient way to tune the optical properties of OLEDs without significant affecting the other electrical properties, such as the internal electrical field and the width and location of the recombination zone. We anticipate the results reported herein might open a new avenue toward higher device performance.

Acknowledgements

We thank the Ministry of Science and Technology of Taiwan (Grant Nos.: NSC 102-ET-E-009-005, NSC 103-2923-E-009-001-MY3, and NSC 101-2628-E-009-008-MY3) and the Ministry of Education of Taiwan (through the ATU program) for financial support.

References

[1] B.W. D'Andrade, S.R. Forrest, Adv. Mater. 16 (2004) 1585–1595.
[2] H.B. Wu, J.H. Zou, F. Liu, L. Wang, A. Mikhailovsky, G.C. Bazan, W. Yang, Y. Cao, Adv. Mater. 20 (2008) 696–702.
[3] S. Reineke, F. Lindner, G. Schwartz, N. Seidler, K. Walzer, B. Lüssem, K. Leo, Nature 459 (2009) 234–238.
[4] C. Adachi, M.A. Baldo, M.E. Thompson, S.R. Forrest, J. Appl. Phys. 90 (2001) 5048–5051.
[5] E.L. Williams, K. Haavisto, J. Li, G.E. Jabbour, Adv. Mater. 19 (2007) 197–202.
[6] N.C. Greenham, R.H. Friend, D.C. Bradley, Adv. Mater. 6 (1994) 491–494.
[7] T. Nakamura, N. Tsutsumi, Noriyuki, H. Fujii, J. Appl. Phys. 97 (2005) 054505.
[8] C.F. Madigan, M.-H. Lu, J.C. Sturm, Appl. Phys. Lett. 76 (2000) 1650–1652.
[9] W.K. Huang, W.S. Wang, H.C. Kan, F.C. Chen, Jap. J. Appl. Phys. 45 (2006) L1100–L1102.
[10] L. Petti, M. Rippa, R. Capasso, G. Nenna, A.D.G.D. Mauro, M.G. Maglione, C. Minarini, Nanotechnology 24 (2013) 215206.
[11] J. Feng, T. Okamoto, Opt. Lett. 30 (2005) 2302–2304.
[12] V. Bulović, V.B. Khalfin, G. Gu, P.E. Burrows, D.Z. Garbuzov, S.R. Forrest, Phys. Rev. B 58 (1998) 3730–3740.
[13] J. Lee, N. Chopra, F. So, Appl. Phys. Lett. 92 (2008) 033303.
[14] R.H. Jordan, A. Dodabalapur, R.E. Slusher, Appl. Phys. Lett. 69 (1996) 1997–1999.
[15] J. Lee, N. Chopra, D. Bera, S. Maslov, S.H. Eom, Y. Zheng, P. Holloway, J. Xue, F. So, Adv. Energy Mater. 1 (2011) 174–178.
[16] C.L. Lin, H.C. Chang, K.C. Tien, C.C. Wu, Appl. Phys. Lett. 90 (2007) 071111.
[17] A. Dodabalapur, L.J. Rothberg, R.H. Jordan, T.M. Miller, R.E. Slusher, J.M. Philips, J. Appl. Phys. 80 (1996) 6954–6964.
[18] S.K. So, W.K. Choi, L.M. Leung, K. Neyts, Appl. Phys. Lett. 74 (1999) 1939–1941.
[19] H. Rooms, D. Hermes, S. Harkema, C. Tanase, T.V. Mol, P.W.M. Blom, J. Wilson, J. Photon. Energy 1 (2011) 011024.
[20] F.C. Chen, S.C. Chang, G. He, S. Pyo, Y. Yang, M. Kurotaki, J. Kido, J. Polym. Sci. Part B: Polym. Phys. 41 (2003) 2681–2690.
[21] F.C. Chen, S.C. Chien, Y.S. Chen, Appl. Phys. Lett. 94 (2009) 043306.
[22] F.C. Chen, S.C. Chien, S.W. Lee, Electrochem. Solid-State Lett. 11 (2008) J50–J53.
[23] K.A. Neyts, J. Opt. Soc. Am. A 15 (1998) 962–971.
[24] S.A. Ahkmanov, S.Y. Nikitin (Eds.), Physical Optics, Oxford University, 1997.
[25] S.Y. Kim, W.I. Jeong, C. Mayr, Y.S. Park, K.H. Kim, J.H. Lee, C.K. Moon, W. Brütting, J.J. Kim, Adv. Funct. Mater. 23 (2013) 3896–3900.
[26] K.H. Kim, C.K. Moon, J.H. Lee, S.Y. Kim, J.J. Kim, Adv. Mater. 26 (2014) 3844–3847.